Published in final edited form as:
Comput Biol Med. 2008 ; 38(11-12): 1140–1151. doi:10.1016/j.compbiomed.2008.08.010.

Tachycardia-induced early afterdepolarizations: insights into potential ionic mechanisms from computer simulations

Ray B. Huffaker[1], **Richard Samade**[2], **James N. Weiss**[3], and **Boris Kogan**[1]

[1] Department of Computer Science, University of California, Los Angeles

[2] Department of Bioengineering, University of California, Los Angeles

[3] Cardiovascular Research Laboratory, Department of Medicine (Cardiology), David Geffen School of Medicine at UCLA, Los Angeles, California

Abstract

Although early afterdepolarizations (EADs) are classically thought to occur at slow heart rates, mounting evidence suggests that EADs may also occur at rapid heart rates produced by tachyarrhythmias, due to Ca overload of the sarcoplasmic reticulum (SR) leading to spontaneous SR Ca release. We hypothesized that the mechanism of tachycardia-induced EADs depends on the spatial and temporal morphology of spontaneous SR Ca release, and tested this hypothesis in computer simulations using a ventricular action potential mathematical model. Using two previously suggested spontaneous release morphologies, we found two distinct tachycardia-induced EAD mechanisms: one mechanistically similar to bradycardia-induced EADs, the other to delayed afterdepolarizations (DADs).

Keywords

early afterdepolarizations; spontaneous release; tachyarrhythmias; computer simulation; mathematical modeling

1. Introduction

Life-threatening cardiac arrhythmias, resulting from abnormal electrical activity in tissue, have been the subject of numerous clinical, physiological, and computational studies. The propagation of electrical excitation in tissue is determined in many respects by processes in individual cells. In particular, the appearance of cellular early afterdepolarizations (EADs) and delayed afterdepolarizations (DADs) are though to exert great influence on electrical behavior at the tissue level. EADs induced by rapid pacing rates, such as those rates associated with ventricular tachycardia, may facilitate the development of more pathological arrhythmias, such as torsades des pointes or ventricular fibrillation.

EADs have classically been described as occurring during bradycardia, under conditions of reduced repolarization reserve caused by drugs [1–3], ion channel mutations [4, 5],

Correspondence to Boris Kogan, UCLA Computer Science Dept., 405 Hilgard Ave, Los Angeles, CA 90095-1596., kogan@cs.ucla.edu, Phone 310-825-7393, Fax 310-825-2273.

remodeling of ion channels [6], or electrolyte abnormalities such as hypokalemia [7]. These bradycardia-induced EADs are generally thought to be due to reduced repolarization reserve allowing regenerative reactivation of the L-type Ca current ($I_{Ca,L}$) in a voltage (V) window within which partial activation and incomplete inactivation of $I_{Ca,L}$ overlap [8]. As $I_{Ca,L}$ reactivates and initiates the EAD upstroke, it secondarily causes a corresponding cytosolic Ca (Ca_i) aftertransient just after the EAD upstroke, mediated by $I_{Ca,L}$–gated Ca-induced Ca release (CICR) from the sarcoplasmic reticulum (SR). In this case, the EAD upstroke occurs before the Ca_i aftertransient. EADs of this type have been termed early EADs [9], since they tend to occur during the plateau phase of the action potential (AP).

However, EADs have also been observed at rapid heart rates (tachycardia), both in experiments [10] and computer simulations [11–13]. Experimental evidence has suggested [14, 15] that these EADs may be generated by spontaneous (i.e. non-$I_{Ca,L}$ gated) release of Ca from the SR occurring during the repolarization phase. In this mechanism, the Ca_i aftertransient occurs first due to SR and cytoplasmic Ca overload triggering spontaneous release, which secondarily triggers the corresponding EAD upstroke by activating inward Ca-sensitive currents to produce a transient inward current (I_{ti}). This is similar to the classic mechanism of DADs, but with spontaneous release occurring during systole (repolarization) instead of diastole [16]. EADs of this type have been termed late EADs [9], since they tend to occur during late repolarization phase, with a lower takeoff potential than early EADs.

Spontaneous SR Ca release is caused by local SR Ca release events that propagate through the cytoplasm as Ca waves [17, 18], suggesting that different patterns of local release may facilitate different global spontaneous release morphology and timing. We hypothesize that the mechanism of tachycardia-induced EADs may depend on the spatial and temporal patterns of spontaneous release waves.

To test this hypothesis, we performed computer simulation of the ventricular AP using a mathematical model [19]. In this model, spontaneous SR Ca release is represented using a modified Hodgkin-Huxley type equation for gating processes. The parameters responsible for spontaneous release kinetics, amplitude, and timing in the AP cycle can be modified to produce a spectrum of patterns. We studied two different patterns, which correspond to two physiologically plausible situations. The first is a low peak amplitude, long duration spontaneous release event [19] that represents spontaneous release initiated at a single site which then propagates slowly through the remainder of the cell. The second is a high amplitude, short duration spontaneous release event [20] that represents spontaneous release initiated near-simultaneously at multiple sites, so that the Ca waves originating at each site rapidly fuse together, abbreviating the duration and increasing the summated amplitude of global Ca release transient.

We found that the mechanism of tachycardia-induced EADs depended on the spontaneous release characteristics. We observed two types of tachycardia-induced EADs, one produced by each spontaneous release pattern, when our model was altered to simulate long QT 1 (LQT1) syndrome. One type of tachycardia-induced EAD, mechanistically similar to early EADs, was associated with the low amplitude, long duration spontaneous release starting during late diastole just before the AP upstroke. The other type, mechanistically similar to late EADs, was caused by the high amplitude, short duration spontaneous release occurring during systole.

We compare these mechanisms to experimental findings and discuss their possible relationships to long QT syndromes (LQTS), as well as to catecholaminergic polymorphic ventricular tachycardia (CPVT) syndromes. Our results provide insights into the potential ionic mechanisms governing the interplay between spontaneous release, DADs and EADs,

which may have important implications for the initiation [21] and perpetuation [11–13] of tachyarrhythmias in cardiac tissue.

2. Methods

In the present study, we utilized the Chudin model of the guinea pig ventricular AP [19]. An AP model does not consider the spatially distributed properties of a real cardiac myocyte, instead averaging cell-wide characteristics. The Chudin model incorporates several properties of Ca dynamics that have been observed in physiological experiments: graded CICR gated by $I_{Ca,L}$ [22], prevention of complete SR depletion during normal CICR [23], accumulation of Ca in the cytosol (Ca_i) and Ca in the junctional SR (Ca_{jsr}) during high-frequency stimulation [24], and spontaneous release (denoted in the model as the Ca^{2+} ion flux J_{spon}) dependent on Ca overload concentrations in both the SR and cytosol [25]. This model has since been modified [26] to reproduce Ca alternans by reformulating CICR as a time dependent process with a steep dependence on Ca_{jsr} (see Shiferaw et al. [27]), while leaving unchanged the above mentioned Ca dynamics properties (for details see Appendix).

The Chudin model was chosen because it can reproduce different J_{spon} wave morphologies, such as those suggested in previous simulations [19, 20], by modifying J_{spon} parameter values. The equation for J_{spon} in the Chudin model is:

$$J_{spon}=G_{spon}p(Ca_{jsr}-Ca_i) \quad \text{(Eq. 1)}$$

G_{spon} = 60 ms^{-1} is the spontaneous release channel conductance. The gate variable p can be considered the probability of J_{spon} occurrence. It is described by a Hodgkin-Huxley type differential equation, though dependent on Ca_i and Ca_{jsr} rather than V. Ca_{jsr}-Ca_i, the Ca^{2+} gradient between the JSR and cytosol, is the chemical driving force.

The differential equation describing the gate variable p is:

$$\frac{dp}{dt}=\frac{p_\infty-p}{\tau_p} \quad \text{(Eq. 2)}$$

$$\tau_p=\tau_1+\tau_2(1-p_\infty) \quad \text{(Eq. 3)}$$

τ_p, the time constant of variable p, effectively determines the duration of a J_{spon} event. If τ_p is increased (by increasing parameters τ_1 and τ_2), the duration of J_{spon} events also increases. p_∞, the steady state value of p, is a bilinear approximation of a Hodgkin-Huxley type sigmoidal function of two variables (Ca_i and Ca_{jsr}), explicitly defined by the following equation (and illustrated in Fig. 1*A*):

$$p_\infty=\begin{cases} 0, & if\ region\ I \\ \frac{Ca_{jsr}-K1}{K3-K1}, & if\ region\ II(a) \\ \left(\frac{Ca_i-K2}{K4-K2}\right)\left(\frac{Ca_{jsr}-K1}{K3-K1}\right), & if\ region\ II(b) \\ \frac{Ca_i-K2}{K4-K2}, & if\ region\ II(c) \\ 1, & if\ region\ III \end{cases} \quad \text{(Eq. 4)}$$

If either Ca_{jsr} or Ca_i are below the lower thresholds set by parameters *K1* and *K2*, respectively, then $p_\infty = 0$ (see Fig. 1 *A*, region I). If both Ca_{jsr} and Ca_i exceed the lower thresholds *K1* and *K2*, but either fails to exceed the upper threshold set by parameters *K3* and *K4*, respectively, then p_∞ is approximated by a linear function of Ca_{jsr} and Ca_i (see Fig. 1 *A*, region II). If both Ca_{jsr} and Ca_i exceed the upper thresholds *K3* and *K4*, then $p_\infty = 1$ (see Fig. 1 *A*, region III).

K1 and *K2* are the threshold for a J_{spon} event to occur. The J_{spon} threshold effectively determines the timing of the onset of J_{spon} events in the AP cycle. During phase 3 and 4 of a normal AP, Ca_{jsr} is increasing and Ca_i is decreasing. Thus, to make J_{spon} start earlier in the AP cycle, *K1* (the Ca_{jsr} threshold) should be decreased and *K2* (the Ca_i threshold) should be increased. Table 1 presents the two pairs of *K1* and *K2* values used in the present study: one pair that leads to J_{spon} events starting during diastole (temporally outside the AP) and the other that leads to J_{spon} events during systole (during the AP).

The differences (*K3*-*K1*) and (*K4*-*K2*) effectively determine the amplitude of a J_{spon} event. If either of the differences are reduced (either by increasing the lower thresholds *K1* and *K2*, or decreasing the upper thresholds *K3* and *K4*), then the slope of the p_∞ function and p_∞ itself are increased, leading to higher-amplitude J_{spon} events.

A desired J_{spon} morphology can be obtained by setting the desired duration (choosing the appropriate value of τ_p) and amplitude (choosing appropriate values of *K3*-*K1* and *K4*-*K2*). Table 2 describes the J_{spon} morphology for two different sets of parameter values used in the AP model for the present study. The first set of parameter values produces relatively low amplitude, long duration J_{spon} events (see Fig. 1 *Bii*), as in [19]. In the second set of parameter values, τ_p is an order of magnitude smaller than in the original, while the differences (*K3*-*K1*) and (*K4*-*K2*) are at least an order of magnitude larger. Thus, it produces high amplitude, short duration J_{spon} events (see Fig. 1 *Bi*), as in [20]. The total Ca in an average release was conserved between morphologies.

By first selecting the timing of the J_{spon} onset in the AP cycle from Table 1 (setting the values of *K1* and *K2*), and then selecting a J_{spon} morphology from Table 2 (setting the values of τ_p, *K3*, and *K4*), we obtained four different J_{spon} events to study: low amplitude, long duration J_{spon} during diastole; low amplitude, long duration J_{spon} during systole; high amplitude, short duration J_{spon} during diastole; and high amplitude, short duration J_{spon} during systole.

The appearance of EADs under conditions of tachycardia in the Chudin AP model was contingent on several factors. The AP model itself needed to be altered to simulate LQT1, which was accomplished by reducing the slow component of the delayed rectifier K current (I_{Ks}) by 54%. This reduces outward current during repolarization, reducing repolarization reserve and prolonging AP duration (APD). With this modification, we induced J_{spon} and EADs by rapid pacing, applying an external stimulus at a high frequency (6.25 Hz, or basic cycle length 160 ms, similar to the rapid pacing rates experienced by individual cells during tachyarrhythmias) to induce Ca accumulation in the cytosol and SR and leading to the appearance of J_{spon}. The train of periodic stimuli was stopped when d*V*/d*t* became positive during repolarization (indicating a potential EAD). Otherwise, the next stimulus would be large enough to elicit a new AP that would overwhelm the potential EAD.

Computer simulations were performed on a desktop computer. The ordinary differential equations were numerically integrated using an explicit Euler method. The time step was dynamically adaptive to rapid changes in *V*, varying between 0.005 and 0.1 ms. Reducing the time step to 0.0005 ms did not significantly alter the results.

3. Results

3.1 Rapid pacing induces spontaneous release

Pacing the AP model at a rapid rate causes accumulation of both Ca_i and Ca_{jsr}. Eventually, Ca_i and Ca_{jsr} reach overload conditions, triggering J_{spon}. The number of paced beats necessary to cause the first J_{spon} event depends primarily on the pacing rate; faster rates cause faster Ca accumulation and hence J_{spon} occurs sooner. J_{spon} temporarily drains Ca_{jsr}, but accumulation resumes with subsequent paced beats and J_{spon} continues to occur with a period that depends primarily on the pacing rate. J_{spon} influences the AP by increasing Ca_i and altering Ca-sensitive membrane currents such as $I_{Ca,L}$, I_{NaCaX} and $I_{ns,Ca}$. As we will show, the induction of EADs by J_{spon} is determined by the J_{spon} morphology and timing of the J_{spon} onset in the AP cycle.

3.2 "Early" EADs caused by a low amplitude, long duration J_{spon} during diastole

When the AP model with the low amplitude, long duration J_{spon} during diastole (see Methods and Tables 1 and 2) is paced at a rate of 160 ms, J_{spon} occurs after approximately 2.4 s (see Fig. 2 *A*, trace of J_{spon}). The J_{spon} onset starts in late diastole just before the start of the new AP cycle (see Fig. 2 *A*, vertical dotted line labeled "J_{spon} onset" illustrates relative timing of J_{spon} onset and AP upstroke). J_{spon} continues through the AP, augmenting the Ca_i transient (see Fig. 2 *A*, compare the results with J_{spon}, solid trace, and the results with J_{spon} manually prevented, dashed trace). Increased Ca_i potentiates Ca-sensitive inward repolarization currents such as I_{NaCaX} and the Ca-activated nonselective cation current ($I_{ns,Ca}$), reducing repolarization reserve enough to produce an overt EAD (see Fig. 2 *A*, trace of *V*). If the diastolic J_{spon} is manually prevented, no EAD occurs (see Fig. 2 *A*, dashed traces).

To determine which current carries the depolarizing charge of the EAD upstroke, we examine the rate of change of the membrane ionic currents immediately before the EAD upstroke (Table 3, row $\dot{I}_{i,EAD}$). The candidate currents are all those reducing repolarization reserve during this time, either increasing inward currents or decreasing outward currents. In either case, the rate of change will be negative, since convention dictates inward currents as negative and outward currents as positive. Four such currents reduce repolarization reserve immediately before the EAD upstroke: increasing inward current $I_{Ca,L}$ and decreasing outward currents I_{Ks}, I_{Kr} (the rapid component of the delayed rectifier K current), and $I_{p(Ca)}$ (the sarcolemmal Ca^{2+} pump current). These candidates can be narrowed down by comparing their rates of change to the rates of change they exhibit during the same phase of repolarization of an AP without an EAD (Table 3, row $\dot{I}_{i,\,noEAD}$). Of the four, only $I_{Ca,L}$ is reducing repolarization reserve more in the EAD case than in the case with no EAD, indicated by the negative value in row $\dot{I}_{i,EAD}; -\dot{I}_{i,\,noEAD}$ of Table 3. Therefore, we conclude $I_{Ca,L}$ is the current responsible for the EAD upstroke (as in early EADs). I_{NaCaX} and $I_{ns,Ca}$ are not causing the EAD upstroke themselves, though they are producing inward current during that time (Table 3, row $\dot{I}_{i,EAD}$). Rather, sustained J_{spon} through the AP potentiates I_{NaCaX} and $I_{ns,Ca}$, contributing to the initial delay of repolarization that then allows $I_{Ca,L}$ reactivation to cause the EAD upstroke.

Examining the EAD closely (see Fig. 2 *B*) confirms the role of $I_{Ca,L}$ as depolarizing charge carrier and determines the relative timing of the EAD upstroke and Ca_i aftertransient. At time $t = 2.500$ s, we find that *V* is decreasing ($dV/dt < 0$), the Ca_i transient is declining ($d(Ca_i)/dt < 0$), and $I_{Ca,L}$ is decreasing ($d(|I_{Ca,L}|)/dt < 0$), indicating normal repolarization. We then find that $I_{Ca,L}$ reactivation ($d(|I_{Ca,L}|)/dt > 0$) occurs at time $t_1 = 2.505$ s, the EAD upstroke ($dV/dt > 0$) occurs next at time $t_2 = 2.538$ s, and the Ca_i aftertransient ($d(Ca_i)/dt > 0$) occurs last at time $t_3 = 2.593$ s. Suppressing $I_{Ca,L}$ reactivation, by manually enforcing a

monotonic decrease of $|I_{Ca,L}|$ beginning at $t = 2.500$ s, eliminates the EAD and Ca_i aftertransient.

The underlying cause of the $I_{Ca,L}$ reactivation is the disparity of the time constants for the activation gate variable, d, and the inactivation gate variable, f, as described by Zeng et al. [28]. During repolarization of an AP with no EAD, the $I_{Ca,L}$ current decreases to 0 as d decreases to 0, closing the activation gate. Meanwhile, f increases to represent recovery from inactivation. When the balance of the currents is altered via J_{spon} and amplified inward Ca-sensitive currents, the AP temporarily enters a long plateau region where V is virtually constant. Since the time constant of d is approximately 50 times faster than the time constant of f for this range of V, d approaches its steady value much faster. V has become virtually constant and so d becomes virtually constant, but f continues to increase since it is slower to reach its steady state. Hence, the product df begins to increase and $I_{Ca,L}$ reactivation occurs.

Low amplitude, long duration J_{spon} occurring during systole or early diastole causes neither EADs nor DADs (as shown later in Fig. 4). The ensuing AP is too delayed for J_{spon} to affect repolarization reserve and produce $I_{Ca,L}$ reactivation, and the low amplitude does not release Ca^{2+} fast enough to cause a Ca_i aftertransient via I_{ti}. Instead, repolarization proceeds as normal.

3.3 “Late” EADs caused by high amplitude, short duration J_{spon} during systole

The AP model was modified to generate a high amplitude, short duration J_{spon}, as in [20] (see Methods and Tables 1 and 2). When paced at a rate of 160 ms, J_{spon} occurs during systole after approximately 1.6 s (see Fig. 3*A*, solid traces). Both an EAD and a Ca_i aftertransient occur in conjunction with the J_{spon}, as well as $I_{Ca,L}$ reactivation. If the J_{spon} event is manually prevented during simulation, no EAD occurs (see Fig. 3*A*, dashed traces).

To determine the mechanism by which J_{spon} causes the EAD, we examined the timing of the EAD closely (see Fig. 3*B*). At time $t = 1.650$ s, repolarization is proceeding normally. Then, at time $t_1 = 1.660$ s, J_{spon} occurs. The Ca_i aftertransient ($d(Ca_i)/dt > 0$) immediately begins, and the magnitude of I_{NaCaX} immediately begins to increase at an accelerated rate. Only later, at time $t_2 = 1.676$ s, do the EAD upstroke and $I_{Ca,L}$ reactivation occur. In this case, the EAD is caused by I_{NaCaX} (as in late EADs) and $I_{Ca,L}$ reactivation is a secondary effect.

Fig. 3 shows that the accelerated I_{NaCaX} increase is in response to the systolic J_{spon}, contributing to a transient inward current (I_{ti}). To determine what other currents may contribute to I_{ti}, we compare the rate of change of the membrane ionic currents immediately before the EAD upstroke to their rate of change during the same phase of repolarization of an AP without an EAD (see Table 4), in the same manner as we did in the previous case. Along with I_{NaCaX}, $I_{ns,Ca}$ is the only other current (disregarding the strictly V-dependent currents) reducing repolarization reserve more in the EAD case than the non-EAD case.

A high amplitude, short duration J_{spon} occurring during diastole after the final paced AP is capable of causing a DAD via the same I_{ti}-mediated mechanism. Depending on the size of J_{spon}, the DAD may exceed membrane excitation threshold and trigger a new AP. High amplitude, short duration J_{spon} occurring during diastole just before the final paced AP can cause neither an EAD nor DAD. There is not enough time for a DAD to occur, since the arrival of the next stimulus interrupts it and produces a full AP. $I_{Ca,L}$ reactivation does not occur and cause an EAD on the ensuing AP, since the short duration of the J_{spon} prevents it from maintaining the potentiated Ca-sensitive inward currents through the repolarization phase.

A summary of the general findings for different J_{spon} formulations and timings of the J_{spon} onset in the AP cycle is presented in Fig. 4.

4. Discussion and Conclusions

EADs and DADs are widely believed to act as triggers in the initiation of tachyarrhythmias [16]. We have shown in our previous computer simulation studies how EADs may potentially sustain and exacerbate already established tachyarrhythmias [11–13]. Despite these important roles, the exact mechanism of EADs, particularly those occurring during tachyarrhythmias, is not known in detail. While spontaneous release is believed to cause EADs and DADs occurring at fast pacing rates [10], a lack of physiological data for the processes underlying spontaneous release prevents a full understanding of this mechanism. Mathematical modeling and computer simulation allow us to explore the effect of different predicted patterns of spontaneous release on tachycardia-induced EADs and delineate possible underlying cellular mechanisms. The results, discussed below, provide a framework for future experimental investigation to determine the physiological mechanisms relating spontaneous release characteristics to EADs, DADs, and triggered activity. Expanding our knowledge about mechanisms at the cellular level may help us better understand arrhythmias at the tissue-level (particularly ventricular fibrillation and defibrillation processes).

4.1 Two types of tachycardia-induced EADs: early and late

As described in [17, 18], spontaneous release in cardiac myocytes results from localized SR Ca release, originating in one or several regions of the cell due to Ca overload conditions, which then propagates via CICR as a Ca wave throughout the remainder of the cytoplasm. We replicate two spontaneous Ca wave morphologies suggested by existing AP models [19, 20]. These morphologies may phenomenologically represent possible types of propagating Ca waves in a cell. A low amplitude, long duration J_{spon} [19] may correspond to a Ca wave originating from a single site in the cell, that then propagates slowly (0.1–0.5 mm/s [24]) to the rest of the cell. A high amplitude, short duration J_{spon} [20] may correspond to a Ca wave originating near-simultaneously from multiple sites in the cell, that then more rapidly reaches the rest of the cell.

By adjusting the timing of these J_{spon} morphologies, we identified two distinct mechanisms for tachycardia-induced EADs (Fig. 4). In the first case, low amplitude, long duration J_{spon} starting during late diastole could cause an EAD on the ensuing AP. The EAD upstroke was caused by $I_{Ca,L}$ reactivation and preceded the Ca_i aftertransient; these have been termed early EADs. To create an EAD, the late diastolic timing of this type of J_{spon} event was critical. If J_{spon} occurred earlier in diastole or during systole, it never caused a frank EAD, although it could influence APD. Moreover, the low peak amplitude of J_{spon} was insufficient to cause a measurable DAD. In the second case, high amplitude, short duration J_{spon} during systole could immediately cause an EAD on the same AP. The Ca_i aftertransient preceded the EAD upstroke, which was caused by I_{ti}; these have been termed late EADs. When this type of J_{spon} event occurred during diastole, it could cause a DAD via the same mechanism. Depending on the size of J_{spon}, the DAD could exceed cell membrane excitation threshold and trigger a new AP.

4.2 Role of repolarization reserve

Fig. 5 presents a flowchart illustrating the similarities and differences between the mechanisms of bradycardia-induced EADs, DADs, and our two types of tachycardia-induced EADs. While EADs are known to occur under conditions of reduced repolarization reserve, such as the various LQT syndromes, they usually require further reduction of

repolarization reserve via rate-dependent mechanisms. Under conditions of bradycardia, repolarization reserve is reduced by more complete deactivation of outward K currents during long diastolic intervals [29]. Under conditions of tachycardia, we found that repolarization reserve is reduced by larger Ca-sensitive inward currents during the AP plateau, which in this model is caused by a larger overall Ca_i transient when the J_{spon}-triggered release summated with the AP-triggered, I_{CaL}-gated CICR. It is possible that a smaller summated Ca_i transient, resulting from a differently timed pre-release of SR Ca by J_{spon}, could also reduce repolarization reserve during the subsequent AP by reducing Ca-induced inactivation of $I_{Ca,L}$ and thereby cause an EAD. However, we did not simulate this case. In either the case of a larger or smaller overall Ca_i transient, the key element is that the J_{spon} induced alteration of the Ca_i transient causes a reduction in repolarization reserve during the subsequent AP, allowing $I_{Ca,L}$ reactivation to induce a*n* early EAD.

In both the bradycardia- and tachycardia-induced cases, reduced repolarization reserve facilitates reactivation of $I_{Ca,L}$ and appearance of an EAD. Both these bradycardia- and tachycardia-induced EADs can be considered early EADs, though the mechanisms causing reduced repolarization reserve are different.

If a high amplitude, short duration J_{spon} is delivered in late diastole, the diastolic peak does not persist long enough to amplify the Ca-sensitive currents during the repolarization phase of the ensuing AP, and an $I_{Ca,L}$ reactivation-induced EAD cannot occur. However, as presented in Fig. 5, the large J_{spon} Ca flux can instantaneously produce a Ca_i aftertransient and I_{ti} that causes an afterdepolarization. Depending on the timing of the J_{spon} event, the afterdepolarization may be a late EAD (if occurring during systole) or a DAD (if occurring during diastole).

4.3 Spontaneous release generating paired DADs and EADs

A shared spontaneous release-dependent mechanism for EADs and DADs has been suggested by both Priori et al. [30] and Volders et al. [14]. These groups found that the β-adrenergic agonist isoproterenol could induce both EADs and DADs in the same myocyte. In particular, they found that EADs and DADs could be associated with the same AP: a "late-coupled" DAD could occur just before (and often be interrupted by) the upstroke of a paced AP that then exhibited an EAD. An obvious mechanism would be two separate J_{spon} events, one J_{spon} peak occurring in diastole and the second in systole. However, our results suggest a more interesting alternative, which depends on an intermediate pattern of spontaneous release between the extremes of the low amplitude, long duration J_{spon} and the high amplitude, short duration J_{spon}. If we amplify the peak of the long duration J_{spon} to an intermediate value between our high and low amplitude cases, a J_{spon} event starting in late diastole is now sufficient to induce a DAD, and the elevation in Ca_i persists long enough to reduce repolarization reserve and cause an early EAD in the subsequent AP (Fig. 6*A*), reproducing late-coupled DADs similar to those observed in the physiological experiments [14, 30]. A single J_{spon} event starting in diastole explaining both the DAD and EAD may be more plausible, as two separate J_{spon} events occurring so temporally close to one another may be unlikely. Amplifying the J_{spon} peak further, but still considerably smaller than the high amplitude case, we observe a DAD that itself triggers an AP with an early EAD (Fig. 6*B*), reproducing another phenomenon observed in the data of Priori et al. [30]. Thus, our simulation results can reproduce (see Fig. 6) observed physiological phenomena [14, 30] and suggest alternative, more parsimonious explanations.

4.5 Limitations and clinical implications

Although computer modeling is a powerful tool for predicting and identifying novel cardiac arrhythmia mechanisms, the relationship to real cardiac arrhythmias cannot be established

without solid experimental confirmation. In particular, it will be especially important to establish direct relationships between Ca phenomena in spatially distributed cardiac cells and the phenomena observed with our spatially averaged AP model. However, it is encouraging that our simulations have replicated a number of experimentally observed afterdepolarization phenomena [14, 30]. Further work will be necessary to determine whether both EAD mechanisms are physiologically relevant. Until the development of required physiological imaging technology, our results based on previously introduced spontaneous release morphologies may be considered mathematical modeling predictions. In the mean time, as a preliminary speculation, it might hypothesized that when excitation-contraction features are relatively normal, such as in LQTS, spontaneous release may be more likely to occur in diastole when the luminal SR Ca content is highest and ryanodine receptor excitability is most recovered, favoring the early EAD mechanism. Conversely, when excitation-contraction coupling exhibits accelerated recovery of ryanodine receptor excitability, such as in CPVT syndromes and heart failure [31], spontaneous release during systole may become more likely, promoting the late EAD mechanism, especially if spontaneous release were initiated from multiple sites.

Arrhythmias in LQT1 are potentiated by sympathetic stimulation [32]. In our previous simulation studies we found that although EADs occurred during reentry in LQT1 tissue, they were not able to induce triggered activity unless paired with a moderate increase in sympathetic tone [12]. The increased sympathetic tone potentiates Ca cycling, acceleration Ca accumulation and leading to more powerful J_{spon} and consequently more powerful EADs [33].

In the present study we simulated LQT1, but our previous tissue simulations strongly suggest these results are generalizable to a number of physiologically relevant conditions. The appearance of tachycardia-induced early EADs during reentrant tachycardia was shown for both simulated LQT1 (caused by reduced I_{Ks}) and LQT2 (caused by reduced I_{Kr}), with qualitatively similar effects on wave propagation [12]. We would expect the same results in virtually any ionic model with reduced repolarization reserve and uninhibited Ca cycling, whether due to reduced K current (LQT1,2), incomplete Na current inactivation (LQT3), or increased sensitivity of inward repolarization currents to elevated Ca_i [13].

We have also shown in tissue studies that our results are generalizable to different cell types. The true myocardium is heterogeneous with respect to repolarization reserve and Ca cycling, both transmurally and base-to-apex [34–36]. We have shown in transmurally heterogeneous 3-dimensional tissue studies that regions of relatively reduced repolarization reserve (such as mid-myocardial M-cells) were more prone to our tachycardia-induced early EADs [33].

In our AP model, all ion channel gating processes were represented with a Hodgkin-Huxley type formulation of independent gating variables. A Markovian approach to gating processes introduces interdependent gate variables (channel state probabilities), allowing physiologically realistic representations of individual ion channel gating proteins and direct simulation of channel protein mutations. Markovian representations of several important cardiac ion channels have been introduced in previous studies [4, 37]. We chose not to use Markovian models because they require a significant increase in computational complexity. Furthermore, our experience has shown that introducing Markovian representations for single channels alters the quantitative results for the channel, but does not change the qualitative behaviors [38].

5. Summary

Early afterdepolarizations (EADs) are thought to be an important cause of ventricular arrhythmias in genetic channelopathies, drug reactions, and heart failure. Classically observed at slow heart rates, EADs can also be induced by rapid heart rates, exacerbated by conditions promoting Ca overload in the SR and cytoplasm, and subsequent spontaneous release. To explore possible underlying ionic mechanisms of these EADs, we performed computer simulations using a ventricular action potential mathematical model. We determined how changing model parameters, replicating patterns of spontaneous release amplitude and timing suggested by previous studies, affected EAD formation. We found that: 1) During tachycardia, spontaneous SR Ca release can generate both EADs and DADs. Depending on the morphology and timing of spontaneous release, EADs can be produced via two distinct mechanisms that previously have been termed early and late. 2) Early EADs are caused by low amplitude, long duration spontaneous release starting in late diastole just before the ensuing paced AP. The EAD upstroke is generated by reactivation of window $I_{Ca,L}$, mechanistically similar to bradycardia-induced EADs. 3) Late EADs are more likely to be caused by high amplitude, short duration spontaneous release occurring in systole. The EAD upstroke is generated by a spontaneous release-induced transient inward current (carried by I_{NaCaX} and $I_{ns,Ca}$), mechanistically similar to DADs. 4) A single medium amplitude, long duration spontaneous release starting in late diastole can produce both a DAD and an early EAD on the subsequent paced AP. Increasing spontaneous release amplitude slightly further can produce a DAD that triggers an AP that then exhibits an early EAD. These results coincide with experimental data and suggest a novel explanation.

Acknowledgments

Grants

This work was supported in part by National Heart, Lung, and Blood Institute Program Project Grant P01 HL-078931, by the Laubisch and Kawata Endowments, and by the Ruth L. Kirschstein National Research Service Award GM008185 from the National Institutes of General Medical Sciences.

References

1. Brachmann J, Scherlag BJ, Rosenshtraukh LV, Lazzara R. Bradycardia-dependent triggered activity: relevance to drug-induced multiform ventricular tachycardia. Circulation. 1983; 68:846–856. [PubMed: 6616779]
2. Sicouri S, Antzelevitch C. Afterdepolarizations and triggered activity develop in a select population of cells (M cells) in canine ventricular myocardium: the effects of acetylstrophanthidin and Bay K 8644. Pacing Clin Electrophysiol. 1991; 14(11 Pt 2):1714–20. [PubMed: 1721163]
3. Luo CH, Rudy Y. A dynamic model of the cardiac ventricular action potential. II. Afterdepolarizations, triggered activity, and potentiation. Circ Res. 1994; 74(6):1097–113. [PubMed: 7514510]
4. Clancy CE, Rudy Y. Linking a genetic defect to its cellular phenotype in a cardiac arrhythmia. Nature. 1999; 400(6744):566–9. [PubMed: 10448858]
5. Clancy CE, Rudy Y. Cellular consequences of HERG mutations in the long QT syndrome: precursors to sudden cardiac death. Cardiovasc Res. 2001; 50(2):301–13. [PubMed: 11334834]
6. Tomaselli GF, Zipes DP. What Causes Sudden Death in Heart Failure? Circ Res. 2004; 95(8):754–763. [PubMed: 15486322]
7. Davidenko JM, Cohen L, Goodrow R, Antzelevitch C. Quinidine-induced action potential prolongation, early afterdepolarizations, and triggered activity in canine Purkinje fibers. Effects of stimulation rate, potassium, and magnesium. Circulation. 1989; 79(3):674–86. [PubMed: 2917391]
8. January CT, Riddle JM. Early afterdepolarizations: mechanism of induction and block. A role for L-type Ca2+ current. Circ Res. 1989; 64(5):977–90. [PubMed: 2468430]

9. Jackman WM, Szabo B, Friday KJ, Margolis PD, Moulton K, Wang X, Patterson E, Lazzara R. Ventricular tachyarrhythmias related to early afterdepolarizations and triggered firing: Relationship to QT interval prolongation and potential therapeutic role for calcium channel blocking agents. J Cardiovasc Electrophysiol. 1990; 1:170–195.
10. Volders PG, Vos MA, Szabo B, Sipido KR, de Groot SH, Gorgels AP, Wellens HJ, Lazzara R. Progress in the understanding of cardiac early afterdepolarizations and torsades de pointes: time to revise current concepts. Cardiovasc Res. 2000; 46(3):376–92. [PubMed: 10912449]
11. Kogan, B.; Lamp, ST.; Weiss, JN. Role of intracellular Ca dynamics in supporting spiral wave propagation. In: Bekey, G.; Kogan, B., editors. Modeling and Simulation. Kluwer Academic Publishers; Boston/London/Dordrecht: 2003. p. 177-193.
12. Huffaker R, Lamp ST, Weiss JN, Kogan B. Intracellular calcium cycling, early afterdepolarizations, and reentry in simulated long QT syndrome. Heart Rhythm. 2004; 1(4):441–8. [PubMed: 15851197]
13. Huffaker RB, Weiss JN, Kogan B. Effects of early afterdepolarizations on reentry in cardiac tissue: a simulation study. Am J Physiol Heart Circ Physiol. 2007; 292(6):H3089–102. [PubMed: 17307992]
14. Volders PG, Kulcsar A, Vos MA, Sipido KR, Wellens HJ, Lazzara R, Szabo B. Similarities between early and delayed afterdepolarizations induced by isoproterenol in canine ventricular myocytes. Cardiovasc Res. 1997; 34(2):348–59. [PubMed: 9205549]
15. Choi BR, Burton F, Salama G. Cytosolic Ca2+ triggers early afterdepolarizations and Torsade de Pointes in rabbit hearts with type 2 long QT syndrome. J Physiol. 2002; 543(Pt 2):615–31. [PubMed: 12205194]
16. Wit, AL.; Rosen, MR. Afterdepolarizations and triggered activity: distinction from automaticity as an arrhythmogenic mechanism. In: Fozzard, HA., et al., editors. The heart and cardiovascular system. Scientific foundations. Raven Press; New York: 1992. p. 2113-2163.
17. Takamatsu T, Wier WG. Calcium waves in mammalian heart: quantification of origin, magnitude, waveform, and velocity. Faseb J. 1990; 4(5):1519–25. [PubMed: 2307330]
18. Cheng H, Lederer MR, Lederer WJ, Cannell MB. Calcium sparks and [Ca2+](i) waves in cardiac myocytes. Amer J Physiol-Cell Physiol. 1996; 39:C148–C159.
19. Chudin E, Goldhaber J, Garfinkel A, Weiss J, Kogan B. Intracellular Ca(2+) dynamics and the stability of ventricular tachycardia. Biophys J. 1999; 77(6):2930–41. [PubMed: 10585917]
20. Luo CH, Rudy Y. A dynamic model of the cardiac ventricular action potential. I. Simulations of ionic currents and concentration changes. Circ Res. 1994; 74(6):1071–96. [PubMed: 7514509]
21. Rubart M, Zipes DP. Mechanisms of sudden cardiac death. J Clin Invest. 2005; 115(9):2305–15. [PubMed: 16138184]
22. Lopez-Lopez JR, Shacklock PS, Balke CW, Wier WG. Local calcium transients triggered by single L-type calcium channel currents in cardiac cells. Science. 1995; 268(5213):1042–5. [PubMed: 7754383]
23. Bassani JW, Yuan W, Bers DM. Fractional SR Ca release is regulated by trigger Ca and SR Ca content in cardiac myocytes. Am J Physiol Cell Physiol. 1995; 268(5):C1313–1319.
24. Bers, D. Excitation-Contraction Coupling and Cardiac Contractile Force. 2. Boston: Kluwer Academic Publishers; 2001. p. 294-300.
25. Stern MD, Capogrossi MC, Lakatta EG. Spontaneous calcium release from the sarcoplasmic reticulum in myocardial cells: mechanisms and consequences. Cell Calcium. 1988; 9(5–6):247–56. [PubMed: 3066490]
26. Samade, R.; Kogan, B. International Conference on Bioinformatics and Computational Biology. Las Vegas, NV: CSREA Press; 2007. Calcium alternans in cardiac cell mathematical models.
27. Shiferaw Y, Watanabe MA, Garfinkel A, Weiss JN, Karma A. Model of intracellular calcium cycling in ventricular myocytes. Biophys J. 2003; 85(6):3666–86. [PubMed: 14645059]
28. Zeng J, Rudy Y. Early afterdepolarizations in cardiac myocytes: mechanism and rate dependence. Biophys J. 1995; 68(3):949–64. [PubMed: 7538806]
29. Rudy Y. Modelling and imaging cardiac repolarization abnormalities. J Intern Med. 2006; 259(1): 91–106. [PubMed: 16336517]

30. Priori SG, Corr PB. Mechanisms underlying early and delayed afterdepolarizations induced by catecholamines. Am J Physiol. 1990; 258(6 Pt 2):H1796–805. [PubMed: 2163219]
31. Wehrens XH, Lehnart SE, Marks AR. Intracellular calcium release and cardiac disease. Annu Rev Physiol. 2005; 67:69–98. [PubMed: 15709953]
32. Shimizu W, Antzelevitch C. Differential Effects of Beta-Adrenergic Agonists and Antagonists in LQT1, LQT2 and LQT3 Models of the Long QT Syndrome. J Am Coll Cardiol. 2000; 35(3):778–786. [PubMed: 10716483]
33. Huffaker, RB. Computer Science. University of California, Los Angeles; Los Angeles, CA: 2008. Tachycardia-Induced Early Afterdepolarizations: Ionic Mechanisms and Effects on Wave Propagation in 1, 2, and 3D Tissue (Computer Simulation Study); p. 137
34. Antzelevitch C, Sicouri S, Litovsky SH, Lukas A, Krishnan SC, Di Diego JM, Gintant GA, Liu DW. Hetergeneity within the ventricular wall. Electrophysiology and pharmacology of epicardial, endocardial, and M cells. Circulation Research. 1991; 69:1427–1449. [PubMed: 1659499]
35. Katra RP, Pruvot E, Laurita KR. Intracellular calcium handling heterogeneities in intact guinea pig hearts. Am J Physiol Heart Circ Physiol. 2004; 286(2):H648–56. [PubMed: 14551057]
36. Pruvot EJ, Katra RP, Rosenbaum DS, Laurita KR. Role of calcium cycling versus restitution in the mechanism of repolarization alternans. Circ Res. 2004; 94(8):1083–90. [PubMed: 15016735]
37. Jafri MS, Rice JJ, Winslow RL. Cardiac Ca2+ dynamics: the roles of ryanodine receptor adaptation and sarcoplasmic reticulum load. Biophys J. 1998; 74(3):1149–68. [PubMed: 9512016]
38. Samade, R.; Kogan, B. METMBS'04. Las Vegas, NV: CSREA Press; 2004. The properties of the cardiac cell mathematical model with the Markovian representation of potassium channel gating processes under high pacing rate (computer simulation study).

Biographies

Ray B. Huffaker was born in Sacramento, CA, USA, in 1979. He received a B.S. in Biochemistry and a B.S. in Mathematics from Washington State University, USA, in 2002. He received an M.S. and Ph.D. in Computer Science from the University of California, Los Angeles, USA, in 2005 and 2008, respectively. His thesis concerned the mathematical modeling and computer simulation of cardiac tissue.

Richard Samade was born in Los Angeles, CA, USA, in 1982. He received a B.S. in Electrical Engineering, with a Biomedical Option, from the University of California, Los Angeles, USA, in 2006 and a M.S., from the same University, in 2006. Since 2006, he has been performing his Ph.D. research in the Biomedical Engineering Department of the same University, on the subject of mathematical modeling and computer simulation of defibrillation.

Dr. James N. Weiss was born in New Jersey, USA, in 1949. He received his AB degree from the Hamilton College in New York in 1971, and his MD degree from the University of Pennsylvania, Philadelphia, USA, in 1975, where he also completed his Internal Medicine Residency. He then completed a Cardiology Fellowship at UCLA School of Medicine in Los Angeles, CA, USA, in 1981, where he has since remained on the faculty. He is currently the Chief of Cardiology and Director of the Cardiovascular Research Laboratory. His research interests focus on arrhythmia and ischemia biology.

Dr. Boris Kogan was born in Kishinev, Moldavia, in 1914. He received his Masters Degree in Automatic Control Science in 1938 from the Electrical Engineering department of Kharkov Polytechnic, USSR, and his Ph.D. in automatic control in 1945 from the Institute of Automation and Telemechanics, Moscow Academy of Sciences, USSR. In 1962 he received the degree of Doctor of Engineering Sciences from the Air Force Military Academy in Moscow, USSR. From 1940 to 1981 he conducted research at the Institute of Control Science, USSR, where in 1956 he founded and directed the computer simulation

laboratory. From 1948 to 1980, he was a full professor working part-time at the Moscow University for Physics and Engineering, USSR, in the Department of Radio-Physics. He arrived at the University of California, Los Angeles, USA, in 1987 as a visiting scholar and has since become an adjunct professor in the Computer Science and Biomedical Engineering Departments. In 2005, the IEEE Control Systems Society held a special history plenary session to honor Dr. Kogan's life's work. His current research interest is mathematical modeling and computer simulation of complex dynamical systems, particularly the application of massively parallel computer systems to simulation of cardiac electrophysiological problems.

Appendix

The implementation of Ca alternans was done in the same manner as in [26] and was based on the original investigation presented in [27], which involved the reformulation of CICR into a time-dependent process:

$$\frac{dJ_{CICR}}{dt} = g_{CICR} P_o P_v (Q(Ca_{jsr}) - Ca_i) - \frac{J_{CICR}}{\tau_{CICR}} \quad \text{(Eq. 5)}$$

with the initial condition $J_{CICR}(t = 0) = 0$. Here, J_{CICR} is the CICR flux from the JSR, $g_{CICR} = 2.0\ \text{ms}^{-1}$ the conductance, and $\tau_{CICR} = 30$ ms is the averaged time constant of Ca sparks throughout the myocyte. The open probability P_o reflects the dependence of CICR on Ca entry via $I_{Ca,L}$ and the probability function P_v represents the voltage dependent nature of CICR. Expressions for both P_o and P_v can be found in the original Chudin model [19]. The term $Q(Ca_{jsr})$ is a function that reproduces the steep dependence of CICR on Ca concentration in the JSR. It is represented by the following piecewise-linear function:

$$Q(Ca_{jsr}) = \begin{cases} 0, & Ca_{jsr} < 0.5mM \\ Ca_{jsr} - 0.5, & 0.5mM \le Ca_{jsr} < 0.9mM \\ \chi(u_{rel} Ca_{jsr} + b_{rel}), & Ca_{jsr} \ge 0.9mM \end{cases} \quad \text{(Eq. 6)}$$

where $u_{rel} = 11.0\ \text{ms}^{-1}$ is the gain of CICR at high JSR loads, $b_{rel} = 10.0$ mM/ms is the point of intersection between the second and third segments of $Q(Ca_{jsr})$, and χ is a parameter found in the original Chudin model [19] that prevents complete depletion of the SR during normal CICR.

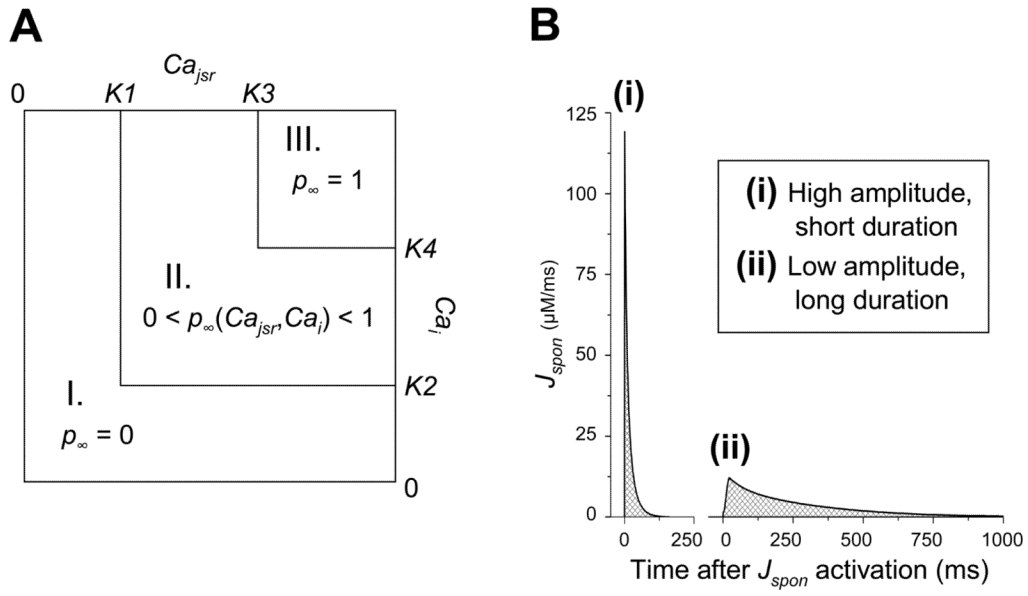

Fig. 1.

Spontaneous release (J_{spon}) formulation. (*A*) Calculation of p_∞, the steady state of the J_{spon} gate variable *p*, as a function of Ca_{jsr} and Ca_i. In region I ($Ca_{jsr} < K1$ or $Ca_i < K2$), $p_\infty = 0$. In region II ($Ca_{jsr} > K1$, $Ca_i > K2$, and either $Ca_{jsr} < K3$ or $Ca_i < K4$), p_∞ is a linear function of Ca_{jsr} and Ca_i. In region III ($Ca_{jsr} > K3$ and $Ca_i > K4$), $p_\infty = 1$. (*B*) Sample traces of J_{spon} activations (elicited via high-frequency stimulation) for two different sets of J_{spon} parameter values. One set (*ii*) yields low amplitude, long duration J_{spon} events. The other set (*i*) yields high amplitude (via reduction of *K3-K1* and *K4-K2*), short duration (via reduction of τ_p) J_{spon} events. The total Ca released from the SR (*crosshatched region*) is relatively equal for both morphologies.

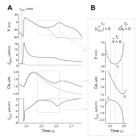

Fig. 2.

A low amplitude, long duration J_{spon} event starting during late diastole causes an $I_{Ca,L}$-induced ("early") EAD. (*A*) Traces of V, J_{spon}, Ca_i, and $I_{Ca,L}$ in time during a tachycardia-induced EAD in an AP model with the low amplitude, long duration J_{spon} (*solid lines*). After stimulating the AP model at a rate of 160 ms for approximately 2.4 s, a large J_{spon} activation starts in late diastole 8 ms before the next paced AP (*vertical dotted line* labeled "J_{spon} onset" indicates start of J_{spon}). An EAD occurs during the repolarization phase of the ensuing AP ($t \approx 2.6$ s), approximately 170 ms after the J_{spon} onset. A Ca_i aftertransient and $I_{Ca,L}$ reactivation are observed in conjunction with the EAD. J_{spon} is small but nonzero during the EAD itself. Dashed traces show the result of preventing the large J_{spon} activation by setting $p_\infty = 0$ just before it would otherwise occur. (*B*) Enlargement of the traces in (*A*) during EAD upstroke, illuminating the exact sequence of events. Time derivatives are denoted with dots (i.e., $dV/dt = \dot{V}$). Slow $I_{Ca,L}$ reactivation (indicated by $d(|I_{Ca,L}|)/dt > 0$) occurs first, at time t_1. The window current increases inward current and reverses repolarization, inducing the V upstroke beginning at time t_2 (indicated by $dV/dt > 0$). The increasing V has a positive feedback effect on $I_{Ca,L}$, causing rapid reactivation and driving a Ca_i upstroke (indicated by $d(Ca_i)/dt > 0$) at time t_3.

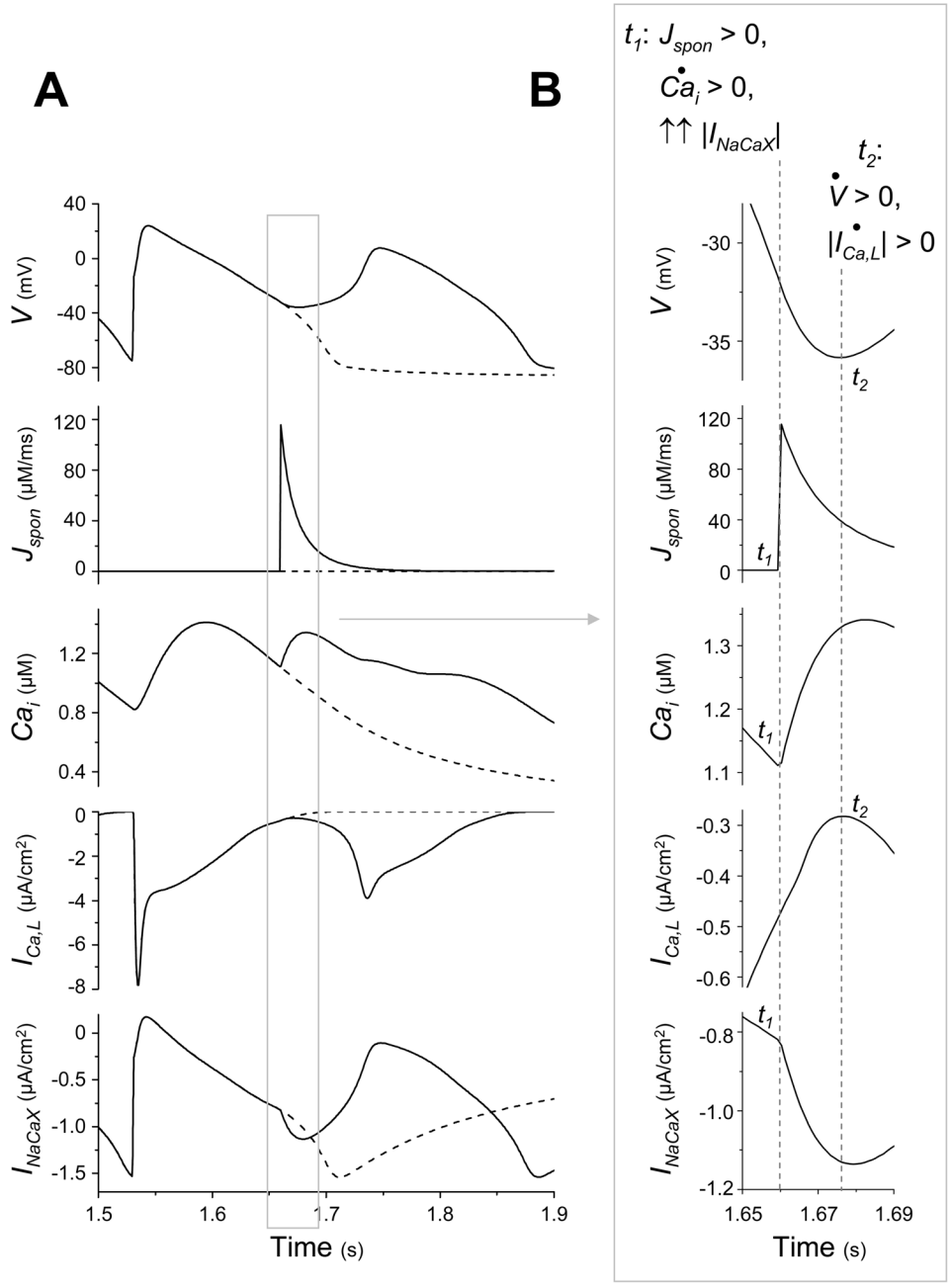

Fig. 3.

A high amplitude, short duration J_{spon} event during systole causes an I_{ti}-induced ("late") EAD. (*A*) Traces of V, J_{spon}, Ca_i, $I_{Ca,L}$, and I_{NaCaX} in time during a tachycardia-induced EAD in an AP model with high amplitude, short duration J_{spon} (*solid lines*). After stimulating the AP model at a rate of 160 ms for approximately 1.5 s, a large J_{spon} activation occurs in systole, during the AP repolarization phase (approximately 1.66 s). An EAD, Ca_i aftertransient, $I_{Ca,L}$ reactivation and sudden increase in I_{NaCaX} are observed in conjunction with the J_{spon} event. Dashed traces show the result of preventing the J_{spon} event by setting $p_\infty = 0$ just before it would otherwise occur. (*B*) Enlargement of the traces in (*A*) during EAD upstroke, illuminating the exact sequence of events. Time derivatives are denoted with

dots (i.e., $dV/dt = \dot{V}$). The large J_{spon} event occurs at time t_1, immediately causing a Ca_i aftertransient (indicated by $d(Ca_i)/dt > 0$). The increased Ca_i causes an immediate increase in reverse-mode I_{NaCaX} activity (and a similar increase in $I_{ns,Ca}$, not shown). This transient inward current, commonly termed I_{ti}, tips the balance of currents and reverses repolarization, inducing the EAD upstroke in V beginning at time t_2 (indicated by $dV/dt > 0$) and associated $I_{Ca,L}$ current. Unlike the previous case, where the EAD upstroke in V drove the Ca_i aftertransient, here the Ca_i aftertransient drives the EAD upstroke in V.

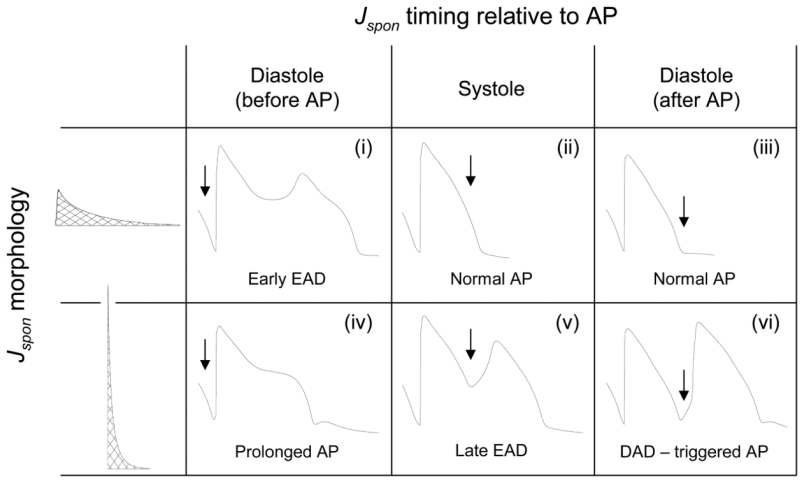

Fig. 4.

Effect of J_{spon} parameter values and timing of the J_{spon} onset in the AP cycle on AP morphology. Table shows representative *V* traces for the two J_{spon} morphologies (low amplitude/long duration versus high amplitude/short duration) and three different times of J_{spon} onset relative to the final paced AP (starting in diastole just before the AP, in systole, and in diastole just after the AP). Arrow indicates exact time J_{spon} onset begins. For the low amplitude/long duration case, J_{spon} in diastole just before the AP can cause an early EAD (*i*), as in Fig. 2. J_{spon} in systole or in diastole just after the AP has no effect on the AP (*ii*,*iii*). For the high amplitude/short duration case, J_{spon} in diastole just before the AP prolongs the AP (*iv*, the DAD in the trace is due to a second, smaller J_{spon} event occurring just after the AP). J_{spon} in systole can cause a late EAD (*v*), as in Fig. 4. J_{spon} in diastole just after the AP can cause a DAD that then triggers a new AP (*vi*).

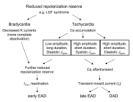

Fig. 5.
Flowchart illustrating the proposed mechanisms for bradycardia-induced EADs, tachycardia-induced EADs, and DADs.

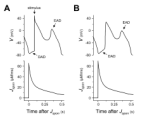

Fig. 6.

Amplified long duration J_{spon} can produce late-coupled DADs and DAD-triggered APs exhibiting EADs. (*A*) J_{spon} conductance is increased in the low amplitude, long duration case to produce a J_{spon} event with long duration and amplitude approximately 47% between the low and high amplitude cases. A single J_{spon} event starting in late diatole elicits an overt DAD that is interrupted by the subsequent paced AP (the pacing stimulus, applied 0.083 s after the J_{spon} onset, is delayed by 75 ms from the normal cycle length to make the DAD more evident). This J_{spon} event also produces an early EAD on the AP. (*B*) J_{spon} conductance increased further to produce a long duration J_{spon} event with amplitude approximately 52% between the low and high amplitude cases. A single J_{spon} event starting in late diastole elicits a suprathreshold DAD that triggers an AP. This J_{spon} event also produces an early EAD on the triggered AP.

Table 1

Timing of the J_{spon} onset in the AP cycle for different J_{spon} thresholds.

***K1* (mM)**	***K2* (μM)**	**Timing of J_{spon} onset**
0.65	0.7	Diastole
0.58	1.12	Systole

Table 2

J_{spon} morphology for two different sets of parameter values.

***K3* - *K1* (mM)**	***K4* - *K2* (μM)**	**τ_p (ms)**	**J_{spon} morphology**
0.5	0.6	$20 + 200(1 - p_\infty)$	Low amplitude, long duration
0.0003	0.08	$20(1 - p_\infty)$	High amplitude, short duration

Table 3

Ionic currents responsible for low amplitude, long duration J_{spon}-induced EAD upstroke. Three calculations of the average rate of change of membrane ionic currents, $\dot{I}_i$ (μA/(cm^2 × s)), over a 35 ms interval: immediately before the EAD upstroke ($\dot{I}_{i,EAD}$), during the same phase of repolarization of an AP without an EAD ($\dot{I}_{i,\ noEAD}$), and the difference between the first two cases ($\dot{I}_{i,EAD} - \dot{I}_{i,\ noEAD}$).

	$\dot{I}_{Na}$	$\dot{I}_{Ca,L}$	$\dot{I}_{Kr}$	$\dot{I}_{Ks}$	$\dot{I}_{NaCaX}$	$\dot{I}_{ns,Ca}$	$\dot{I}_{p(Ca)}$	$\dot{I}_{V}$
$\dot{I}_{i,EAD}$	0	−2.9	−3.1	−2.7	2.0	1.4	−0.9	1.8
$\dot{I}_{i,\ noEAD}$	0	6.6	−5.4	−6.6	−1.6	−5.6	−1.2	16.9
$\dot{I}_{i,EAD} - \dot{I}_{i,\ noEAD}$	0	−9.5	2.3	3.9	3.6	7.0	0.3	−15.1

Table 4

Ionic currents responsible for a high amplitude, short duration J_{spon}-induced EAD upstroke. Three calculations of the average rate of change of membrane ionic currents, $\dot{I}_i$ (μA/(cm^2 × s)), over a 20 ms interval: immediately before the EAD upstroke ($\dot{I}_{i,EAD}$), during the same phase of repolarization of an AP without an EAD ($\dot{I}_{i,\ noEAD}$), and the difference between the first two cases ($\dot{I}_{i,EAD} - \dot{I}_{i,\ noEAD}$).

	$\dot{I}_{Na}$	$\dot{I}_{Ca,L}$	$\dot{I}_{Kr}$	$\dot{I}_{Ks}$	$\dot{I}_{NaCaX}$	$\dot{I}_{ns,Ca}$	$\dot{I}_{p(Ca)}$	$\dot{I}_{V}$
$\dot{I}_{i,EAD}$	0.0	13.2	−8.1	−10.6	−19.5	−43.6	2.6	30.9
$\dot{I}_{i,\ noEAD}$	0.0	12.9	−10.5	−13.7	−8.8	−18.6	−1.1	44.5
$\dot{I}_{i,EAD} - \dot{I}_{i,\ noEAD}$	0.0	0.3	2.5	3.1	−10.8	−25.0	3.7	−13.6